



HAL
open science

Contrasting effects of urban trees on air quality: From the aerodynamic effects in streets to impacts of biogenic emissions in cities

Alice Maison, Lya Lugon, Soo-Jin Park, Christophe Boissard, Aurélien Faucheux, Valérie Gros, Carmen Kalalian, Youngseob Kim, Juliette Leymarie, Jean-Eudes Petit, et al.

► To cite this version:

Alice Maison, Lya Lugon, Soo-Jin Park, Christophe Boissard, Aurélien Faucheux, et al.. Contrasting effects of urban trees on air quality: From the aerodynamic effects in streets to impacts of biogenic emissions in cities. *Science of the Total Environment*, 2024, 946, pp.174116. 10.1016/j.scitotenv.2024.174116 . insu-04622820

HAL Id: insu-04622820

<https://insu.hal.science/insu-04622820v1>

Submitted on 28 Jun 2024

HAL is a multi-disciplinary open access archive for the deposit and dissemination of scientific research documents, whether they are published or not. The documents may come from teaching and research institutions in France or abroad, or from public or private research centers.

L'archive ouverte pluridisciplinaire **HAL**, est destinée au dépôt et à la diffusion de documents scientifiques de niveau recherche, publiés ou non, émanant des établissements d'enseignement et de recherche français ou étrangers, des laboratoires publics ou privés.



Distributed under a Creative Commons Attribution 4.0 International License



Contrasting effects of urban trees on air quality: From the aerodynamic effects in streets to impacts of biogenic emissions in cities

Alice Maison^{a,b,j,*}, Lyà Lugon^a, Soo-Jin Park^a, Christophe Boissard^{c,d}, Aurélien Fauchoux^a, Valérie Gros^c, Carmen Kalalian^{c,i}, Youngseob Kim^a, Juliette Leymarie^e, Jean-Eudes Petit^c, Yelva Roustan^a, Olivier Sanchez^f, Alexis Squarcioni^{a,g}, Myrto Valari^g, Camille Viatte^h, Jérémy Vigneron^f, Andrée Tuzet^b, Karine Sartelet^a

^a CERA, École des Ponts, EDF R&D, IPSL, Marne-la-Vallée 77455, France

^b Université Paris-Saclay, INRAE, AgroParisTech, UMR EcoSys, Palaiseau 91120, France

^c LSCE, CNRS-CEA-UVSQ, IPSL, Gif-sur-Yvette 91191, France

^d Univ Paris Cité and Univ Paris Est Créteil, CNRS, LISA, Paris 75013, France

^e Univ Paris Est Créteil, CNRS, INRAE, IRD, Sorbonne Université, Institut d'Ecologie et des Sciences de L'Environnement de Paris, IEES-Paris, F-94010 Créteil, France

^f Airparif, Association Agréée pour la Surveillance de la Qualité de l'Air en région Île-de-France, 7 rue Crillon, Paris 75004, France

^g Laboratoire de Météorologie Dynamique-IPSL, Sorbonne Université/CNRS/École Normale Supérieure-PSL Université/École Polytechnique-Institut Polytechnique de Paris, Paris 75005, France

^h LATMOS/IPSL, Sorbonne Université, UVSQ, CNRS, Paris 75005, France

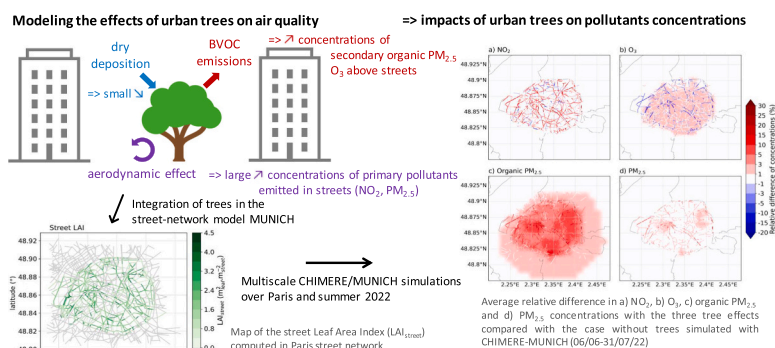
ⁱ Now at Université Paris-Saclay, INRAE, AgroParisTech, UMR EcoSys, Palaiseau 91120, France

^j Now at Laboratoire de Météorologie Dynamique-IPSL, Sorbonne Université/CNRS/École Normale Supérieure-PSL Université/École Polytechnique-Institut Polytechnique de Paris, Paris 75005, France

HIGHLIGHTS

- The aerodynamic effect impacts significantly concentrations of species emitted in streets.
- Biogenic emissions induce mainly an increase in organic particles concentrations.
- Dry deposition on leaves induces a low decrease in gas and particle concentrations.
- Planting of trees with large crowns on high-traffic streets should be avoided.
- Tree species that emit few terpenes should be favored in cities.

GRAPHICAL ABSTRACT



ARTICLE INFO

Editor: Hai Guo

Keywords:
Air-quality modeling

ABSTRACT

Urban trees are often not considered in air-quality models although they can significantly impact the concentrations of pollutants. Gas and particles can deposit on leaf surfaces, lowering their concentrations, but the tree crown aerodynamic effect is antagonist, limiting the dispersion of pollutants in streets. Furthermore, trees emit Biogenic Volatile Organic Compounds (BVOCs) that react with other compounds to form ozone and secondary

* Corresponding author at: CERA, École des Ponts, EDF R&D, IPSL, Marne-la-Vallée, 77455, France.

E-mail address: alice.maison@lmd.ipsl.fr (A. Maison).

<https://doi.org/10.1016/j.scitotenv.2024.174116>

Received 6 April 2024; Received in revised form 16 June 2024; Accepted 16 June 2024

Available online 21 June 2024

0048-9697/© 2024 The Authors. Published by Elsevier B.V. This is an open access article under the CC BY license (<http://creativecommons.org/licenses/by/4.0/>).

Street scale
 Urban trees
 Aerodynamic effect
 Biogenic emissions
 Dry deposition on leaves

organic aerosols. This study aims to quantify the impacts of these three tree effects (dry deposition, aerodynamic effect and BVOC emissions) on air quality from the regional to the street scale over Paris city. Each tree effect is added in the model chain CHIMERE/MUNICH/SSH-aerosol. The tree location and characteristics are determined using the Paris tree inventory, combined with allometric equations. The air-quality simulations are performed over June and July 2022. The results show that the aerodynamic tree effect increases the concentrations of gas and particles emitted in streets, such as NO_x (+4.6 % on average in streets with trees and up to +37 % for NO₂). This effect increases with the tree Leaf Area Index and it is more important in streets with high traffic, suggesting to limit the planting of trees with large crowns on high-traffic streets. The effect of dry deposition of gas and particles on leaves is very limited, reducing the concentrations of O₃ concentrations by -0.6 % on average and at most -2.5 %. Tree biogenic emissions largely increase the isoprene and monoterpene concentrations, bringing the simulated concentrations closer to observations. Over the two-week sensitivity analysis, biogenic emissions induce an increase of O₃, organic particles and PM_{2.5} street concentrations by respectively +1.1, +2.4 and +0.5 % on average over all streets. This concentration increase may reach locally +3.5, +12.3 and +2.9 % respectively for O₃, organic particles and PM_{2.5}, suggesting to prefer the plantation of low-emitting VOC species in cities.

1. Introduction

Trees in urban environments provide numerous benefits to overcome the adverse effects of urbanization (Livesley et al., 2016; Roeland et al., 2019). The city energy and water budgets are strongly influenced by the presence of artificial materials and high buildings and the release of anthropogenic heat. These processes induce an increase in temperature compared to the country side, called the urban heat island (UHI) effect (Nunez and Oke, 1977; Taha, 1997; Arnfield, 2003; Kuttler, 2008; Oke et al., 2017; Masson et al., 2020). Urban air quality is also often deteriorated due to reduced air flows and high local emissions (Lyons et al., 1990; Fenger, 1999; Yang et al., 2020). By creating shade and transpiring, trees improve human thermal comfort and limit the UHI effect (Taleghani, 2018; Hami et al., 2019). They also preserve permeable soils in which runoff water can infiltrate (Livesley et al., 2016; Berland, 2017). While the effects of trees on climate are widely studied in scientific research and known to the general public, the effects on the urban air quality are much less well known. Trees are often promoted for their capacity to remove pollutant from the atmosphere by dry deposition (Nowak et al., 2006; Escobedo and Nowak, 2009; Setälä et al., 2013; Selmi et al., 2016; Xing and Brimblecombe, 2019; Nemitz et al., 2020; Lindén et al., 2023). However, other direct effects are rather negative for air quality. In the street, the tree crowns strongly modify air flows and limit the dispersion of pollutants emitted by traffic (Gromke and Ruck, 2007; Buccolieri et al., 2009; Vos et al., 2013; Jeanjean et al., 2016). Trees naturally emit Biogenic Volatile Organic Compounds (BVOCs) that react with the other compounds of the urban atmosphere to form secondary pollutants such as ozone and secondary organic aerosols (SOAs) (Owen et al., 2003; Calfapietra et al., 2013; Ren et al., 2017). In temperate cities, these effects are mainly present during the vegetative period when trees have leaves. The effect of BVOC emissions, which increases with temperature and light, is expected to be higher in summer and especially during heatwave periods (Niinemets et al., 2004). To estimate the magnitude of these processes, models are useful tools, in particular because they can represent the city heterogeneity, and sensitivity scenarios can be performed to estimate the relative strength of the different tree effects. Computational Fluid Dynamics (CFD) codes are frequently used to study the tree effects on air flows and pollutant concentrations but their fine resolution (~ 1 m) requires high computational resources, limiting the study area to a street or neighborhood and the consideration of complex chemistry (Buccolieri et al., 2011; Santiago et al., 2017; Gromke and Blocken, 2015; Fu et al., 2024). To model air quality at the street scale but over large areas such as cities, parameterized street-network models are developed such as SIRANE (Soulhac et al., 2011, 2012, 2017), the Model of Urban Network of Intersecting Canyons and Highways (MUNICH) (Kim et al., 2018, 2022), OSPM (Berkowicz, 2000) or ADMS-Urban (McHugh et al., 1997; Caruthers et al., 2000; Stocker et al., 2012). They are fast-running codes because air flows are parameterized and streets are considered as an

homogeneous volume or are divided in just a few zones. The aerodynamic effect of trees in street canyons has been parameterized in the street-network model MUNICH based on CFD simulations (Maison et al., 2022a, 2022b). It is coupled to the regional-scale Chemistry-Transport Model (CTM) CHIMERE, with an eulerian approach, allowing to fully represent the formation of secondary pollutants from the regional scale down to the street scale.

The objective of the present study is to estimate the impacts of urban trees on gas and aerosol concentrations. Trees are often considered to be beneficial in improving street air quality because they increase the surface area of deposits, and they also absorb carbon dioxide. It is only more recently that their impact on atmospheric chemistry (Maison et al., 2024) and the trapping of pollutants emitted into the streets (aerodynamic effect, Vos et al. (2013)) has been examined. However, urban trees outside large parks are usually not taken into account in air-quality models, because of the lack of tree inventories that include tree locations and characteristics. To quantify the tree effects, the city of Paris is a relevant place to study because it integrates a detailed tree inventory. Furthermore, Paris is dense, sprawling and regularly subject to air-quality issues. The city is also rather well vegetated, with >200,000 trees in the streets and green spaces and >300,000 trees in the Boulogne and Vincennes woods (<https://www.paris.fr/pages/l-arbre-a-paris-199>, last accessed on 27/02/2024, in French). In this study, each tree effect (aerodynamic effect, dry deposition on leaves, biogenic emissions) is activated one by one in the simulations to quantify their individual impact, or all at once to quantify the overall tree impact in the city of Paris.

First, Section 2 presents the materials and methods. The modeling chain set-up including the input data, and the reference simulation performed without tree are presented in Section 2.1. Section 2.2 describes the integration of the tree effects in the modeling chain. The tree inventory of the Municipality of Paris (Municipality of Paris, 2023) is used to integrate trees in the Paris street network and is combined with allometric equations to estimate tree characteristics (leaf area, dry biomass, tree dimension). The parameterization of the tree aerodynamic effect, previously developed, is applied to the whole city of Paris. Dry deposition of gas and aerosols on both street and tree leaf surfaces is computed based on parameterizations of the literature. Biogenic emissions are estimated from the calculated leaf dry biomass of each individual tree, the tree-species dependent emission factors available in the Model of Emissions of Gases and Aerosols from Nature, MEGANv3.2, and the activity factors of Guenther et al. (1995, 2012) which depends on meteorological conditions. CHIMERE/MUNICH simulations are performed over Paris region and the Paris street network for June and July 2022 with the different tree effects added individually and overall. The impacts on isoprene (C₅H₈), monoterpene, nitrogen dioxide (NO₂), ozone (O₃), organic matter (OM) and particulate matter (PM_{2.5}) concentrations are presented in Section 3.

2. Materials and methods

2.1. Description of the reference simulation

2.1.1. Presentation of the modeling chain CHIMERE/MUNICH

The CTM CHIMERE is used to estimate the urban background concentrations (Menut et al., 2021). It is coupled to the gas-phase mechanism MELCHIOR2, to the aerosol model SSH-aerosol (Sartelet et al., 2020), and to the meteorological model WRF (Powers et al., 2017; Menut et al., 2021), where a one-layer urban canopy model is used (Kusaka et al., 2001), with a prescribed anthropogenic heat flux (Pigeon et al., 2007; Sailor et al., 2015), as described in (Maison et al., 2024). The WRF-CHIMERE domain has a spatial resolution of $1 \text{ km} \times 1 \text{ km}$ and extends from 48.1203°N to 49.2503°N in latitude and from 1.4481°E to 3.5817°E in longitude (see Maison et al. (2024), for a detailed description of the simulations). A time step of 600 s is used for transport, gaseous chemistry and aerosol dynamics are computed with an adaptive time step. MUNICH is a street-network model that simulates with an eulerian approach, gas and particle concentrations at the street level (Kim et al., 2022). To be able to simulate concentrations at the street level and over large areas such as cities, each street is considered as an homogeneous volume. So within a street segment, buildings have the same height (H), and the street width (W) is taken as constant. Streets can have various lengths (L) and are linked by punctual intersections. The MUNICH street network extends from 48.8013°N to 48.9227°N in latitude and from 2.2301°E to 2.4590°E in longitude. MUNICH includes the main processes affecting street concentrations: emission of gas and particles by traffic, horizontal transport by advection between the streets, vertical transport between the street and the background, dry and wet deposition of gas and aerosols, gas chemistry and aerosols dynamics. The model runs with an adaptive time step for transport, gaseous chemistry and aerosol dynamics. MUNICH is one-way coupled to the CTM CHIMERE. Both MUNICH and CHIMERE coupled with WRF (CHIMERE-WRF) are eulerian models, and CHIMERE-WRF is used to estimate the boundary conditions of MUNICH, i.e. meteorological fields and background concentrations above the street. As CHIMERE and MUNICH use the same gas-phase chemistry MELCHIOR2 and aerosol model SSH-aerosol, primary and secondary pollutant concentrations are represented consistently from street to regional scale. The input data used in this study are presented in the following sections with a focus on tree characteristics in Section 2.2.

2.1.2. Paris street network

The Paris street network used in the study is composed of 4655 streets and 3040 intersections. It includes the main streets of the Paris city and the close suburbs (Fig. S1). It has been constructed from the BDTOPO database, available at <https://geoservices.ign.fr/bdtopo> (last accessed on 27/02/2024), the Paris database available at <https://www.data.gouv.fr/fr/datasets/trottoirs-des-rues-de-paris-prs/> (last accessed on 27/02/2024) (Lugon et al., 2020) and the emission inventory provided by Airparif, the air-quality monitoring association for the Île-de-France region. The average street aspect ratio is $H/W = 0.79$. This street aspect ratio is rather homogeneous in Paris (between 0.66 and 2), as shown in Fig. S1, with more opened areas along the Seine river, the ring road and the Vincennes and Boulogne woods. Streets with higher aspect ratio can be found in the Défense district.

2.1.3. Anthropogenic and biogenic emissions

Anthropogenic emission inventory for all activity sectors were provided by Airparif. For sectors other than traffic, the inventory represents the year 2019 with a spatial resolution of $1 \text{ km} \times 1 \text{ km}$. For traffic, emissions are those of June and July 2022, they are given by street segment and are estimated from traffic counting. Biogenic emissions at the regional scale are estimated using MEGANv2.1 in CHIMERE using the land-use approach. At the urban scale in Paris, biogenic emissions are calculated from the Paris tree inventory, as described in Maison et al.

(2024). Special treatments, as detailed below, are necessary to include the trees in the street network used in MUNICH.

2.2. Integration of the tree effects in MUNICH

2.2.1. Integration of trees in the Paris street network

As presented in Maison et al. (2024), the Paris tree inventory, including tree location, species and dimensions is used (Municipality of Paris (2023), March 2023 version). To locate the trees in the street network, streets are considered as rectangles of known four extremity coordinates, and trees are located into the street segments by comparing their coordinates with those of streets. Because of uncertainty about street widths, trees within a perimeter of half of the street width on each side of the street are integrated into the street segment. On the 112,154 roadside trees listed in the Paris tree inventory, 58.6 % are integrated in the MUNICH street network of which 38.8 % in the exact street width and 19.8 % by widening the street width between 1.2 (+20 %) and $2 \times W$ (+100 %) (see Fig. S2). The non-integration of some trees into the street network is mainly due to the fact that they are located in secondary streets that are not included in the network, and also because of inaccuracies in the layout and width of streets, as shown in Figs. S2 and S3. Finally, 36.4 % of the streets in the network contain at least one tree. Although <40 % of the streets had at least one tree associated with them, a significant effect was subsequently observed in our study.

Moreover, the municipality of Paris estimates that 30 % of the trees in the city of Paris are not listed in the database, these missing trees are most likely located in private parks and yards. Roadside trees are rather well documented. The effects of roadside trees that are not integrated in the network are not considered at the street level. However their biogenic emissions are taken into account in the regional-scale simulations to estimate background concentrations (see Section 2.2.4 and Maison et al. (2024)). Note also that trees planted on roofs are not considered here, since their number is very small in Paris compared to roadside and park trees (Méziani et al., 2013) and they are not included in the Paris tree inventory.

The tree characteristics needed to compute the different tree effects at the street level (leaf area, dry biomass and tree crown height) are estimated, as in Maison et al. (2024), based on the Paris Tree inventory and a set of allometric equations from McPherson et al. (2016). The canopy characteristics of each street segment take into account all the trees included in the segment. Depending on the nature of the characteristics, they are averaged or summed over the trees of the street segment. The street Leaf Area Index (LAI_{street} in $\text{m}_{\text{leaf}}^2 \cdot \text{m}_{\text{street}}^{-2}$) and dry biomass (DB in g of dry weight) are computed by summing the leaf areas and dry biomass of all trees included in the same street segment. The top tree height is taken from the Paris tree inventory and is averaged to obtain the street average top tree height (h_{max} in m). More details about the tree characteristic computation can be found in Section S1. The street leaf area index, normalized dry biomass and crown height to building height ratios obtained are plotted for the street network in Fig. S4.

2.2.2. Tree aerodynamic effect

The presence of trees in the street strongly modifies air flows, limiting the dispersion of gaseous and particulate pollutants emitted by traffic. These effects are complex and impact advection and vertical transport, they were studied in detail in Gromke and Ruck (2007); Buccolieri et al. (2009); Vos et al. (2013) and Maison et al. (2022b). The tree aerodynamic effect, i.e. the modification of air flows at the street level by tree crowns, has been parameterized in MUNICH using empirical equations based on CFD simulations (Maison et al., 2022a, 2022b). The vertical profile of horizontal wind speed in the street and the vertical transfer coefficient between the street and the background are parameterized depending on LAI_{street} and on the average top tree crown height to building height ratio h_{max}/H . The tree aerodynamic effect is

expected to be higher in the streets of high LAI_{street} and high h_{max}/H .

2.2.3. Computation of dry deposition on street surfaces and tree leaves

The ability of trees to reduce air pollutant concentrations via dry deposition is often promoted. However in the literature, the amplitude of this process varies (Nowak et al., 2006; Escobedo and Nowak, 2009; Setälä et al., 2013; Selmi et al., 2016; Xing and Brimblecombe, 2019; Nemitz et al., 2020; Lindén et al., 2023), with sometimes highly simplified representations of pollutant deposition rates. To try to estimate if this process modifies significantly the street concentrations, the dry deposition flux of gas and particles is taken into account in the street mass budget. The deposition fluxes are computed as the product of surface area, deposition velocity and average street concentration. Deposition velocities are calculated for each surface (wall, street surface, tree leaf), which is considered homogeneous. A resistive scheme (Fig. S5) is used to compute the deposition velocities, and the different resistances are estimated using equations from the literature (Hicks et al. (1987); Walmsley and Wesely (1996); Wesely (1989); Venkatram and Pleim (1999); Zhang et al. (2002, 2003) for gas and Zhang et al. (2001) for aerosols). Due to their different physico-chemical properties, the parameterizations varies according to the type of compound. The methodology used and the resistance and coefficient formulations taken from the literature are presented in Sections S2 for gas and S3 for particles. Concerning the deposition of BVOCs, due to the lack of measurements to estimate the deposition model parameters, BVOC deposition on street and tree leaf surfaces is not considered. Indeed, several studies suggest that isoprene and monoterpenes are not directly deposited but are rapidly oxidized in the atmosphere and are therefore indirectly deposited as oxygenated VOCs (Karl et al., 2010; Nguyen et al., 2015; Canaval et al., 2020).

2.2.4. Biogenic emissions

The biogenic emissions are computed with the same empirical approach used in Maison et al. (2024). At the regional scale, the biogenic emissions are estimated from the dry biomass of each tree and are then aggregated over the grid cells of the simulation domain. At the street scale, the dry biomass of the trees included in a same street is summed to compute the total dry biomass for each street (eq. (S2)). The street leaf dry biomass computed for the Paris street network is presented in Fig. S4b.

As in Maison et al. (2024), the tree species emission factors are taken from MEGANv3.2 (<https://bai.ess.uci.edu/megan/data-and-code/megan32>, last accessed on 10/07/2023). At the street scale, the activity factors are computed with equations from Guenther et al. (2012) for the temperature effect and from Guenther et al. (1995) for the light effect. The leaf surface temperature is approximated by the air temperature at 2 m simulated by WRF and the Photosynthetic Photon Flux Density (PPFD) is computed from the global solar radiation (SW_2) as: $PPFD = 4.5 \times 0.5 \times SW_g$. These two factors include the selection of the 400–700 nm spectral range of the solar radiation and the conversion of $W.m^{-2}$ into $\mu mol.m^{-2}.s^{-1}$ (Meek et al., 1984). For each street, the temperature and global solar radiation are taken from the CHIMERE-WRF horizontal cell which is located above the middle of the street. The meteorological variables simulated by WRF were compared with data from several weather stations in the Île-de-France region in Maison et al. (2024). In addition, the air temperature (T_{air}) and the global solar radiation that are used in the computation of the BVOC emissions at the street level are compared to measurements performed in the Hôtel de Ville station (HdV) (48.85574°N, 2.35191°E) and in the Qualair platform (48.84638°N, 2.35598°E) (see Fig. S1) in Section S4.

Fairly significant assumptions are made in calculating biogenic emissions, notably that leaf surface temperature is equal to air temperature. The solar radiation reaching the leaves is assumed to be equal to the incoming solar radiation above the street, neglecting the effects of reflections between street surfaces and building shading. The effect of

water stress, which can reduce isoprene emissions (Guenther et al., 2012; Bonn et al., 2019; Otu-Larbi et al., 2020), is not considered here, due to the lack of a precise water balance for calculating soil water content in the model. It should be also noted that biogenic emissions from other tree organs (trunk, branches, flowers, etc.) or from the soil, although significant at certain times of the year (Baghi et al., 2012), are minor for the simulated period compared to leaf emissions and are not considered.

As in CHIMERE regional-scale simulations, the emitted biogenic species are speciated and aggregated into MELCHIOR2 model species. Biogenic species include isoprene, monoterpenes, sesquiterpenes and many other BVOCs (OVOCs), mainly oxygenated compounds, such as methanol, acetone, acetaldehyde and formaldehyde. Note that nitrogen monoxide (NO) and carbon monoxide (CO), which are not BVOCs, are also emitted by trees and considered in the model. The emission maps of isoprene and monoterpenes are shown in Fig. 1. Emissions maps of other species are presented in Fig. S7 and the temporal variation of the different biogenic species are shown in Fig. S8.

Similarly to Maison et al. (2024), isoprene is the most emitted biogenic species with 54.7 % of the total emissions (in mass) following by other oxygenated BVOCs (36.7 %), CO (4.0 %), monoterpenes (3.2 %), sesquiterpenes (0.8 %) and NO (0.5 %). Figs. 1 and S7 show that higher emissions are observed in the streets containing trees and the density of the emissions depends on the quantity of leaf dry biomass and also on tree species via the emission factors.

2.3. Simulation set-up

CHIMERE/MUNICH simulations are performed over the Paris street network from June 1 to July 31. A spin-up period of 5 days is considered, and the results are analyzed starting from June 6. As a reference and for comparison, a simulation without tree is performed (see Section 3.1). Simulations with all tree effects are performed to quantify the overall effect. Specific effects of trees on concentrations are also assessed using shorter simulations (2 weeks). The performed simulations are described in Table 1. As explained in Maison et al. (2024), to quantify the impacts of uncertainties in the emission factors of terpenes, simulations are also performed with a TX2 scenario (Table 1), where monoterpene and sesquiterpene emissions are doubled.

To assess the model's performance, simulated street-level concentrations are compared to measurements, as described in the next section.

2.3.1. Description of the experimental measurements

Concentrations have been measured in the Paris HdV station and in Airparif traffic stations located inside the Paris city or in very near suburbs. These latter correspond to 10 permanent air-quality monitoring stations included within a large operational stations network operated by Airparif. The Paris HdV station was implemented as part of the Impact of sTress on uRban trEEs and on city air quality (sTREET) project. It was located in a small garden, next to the town hall and directly overlooking the quays of the Seine, which is a major road traffic artery. In HdV station, NO_x concentrations in the ambient air were measured using an instrument based on chemiluminescence and VOCs with a Proton Transfer Reaction - Time-Of-Flight - Mass Spectrometry (1000-PTR-TOF-MS) instrument. Concentrations of organic aerosols below 2.5 μm are estimated by using a Quadripole Aerosol Chemical Speciation Monitor (Q-ACSM, Ng et al. (2011)), equipped with a PM_{2.5} lens Xu et al. (2017) and a capture vaporizer.

Note that NO₂ concentrations measured in traffic-type stations vary from 3.7 to 196.7 $\mu g.m^{-3}$ with an average value of 40.9 $\mu g.m^{-3}$. For PM_{2.5}, concentrations vary from 0.4 to 63.2 $\mu g.m^{-3}$ with an average value of 11.2 $\mu g.m^{-3}$. Organic PM_{2.5} concentrations vary from 0.6 to 27.7 $\mu g.m^{-3}$ with an average value of 6.3 $\mu g.m^{-3}$. A concentration peak of organic particles is observed between the 16 and 18th of June due to higher temperatures. More details on the measurements performed can be found in Section S6 of the supplementary materials. The list of

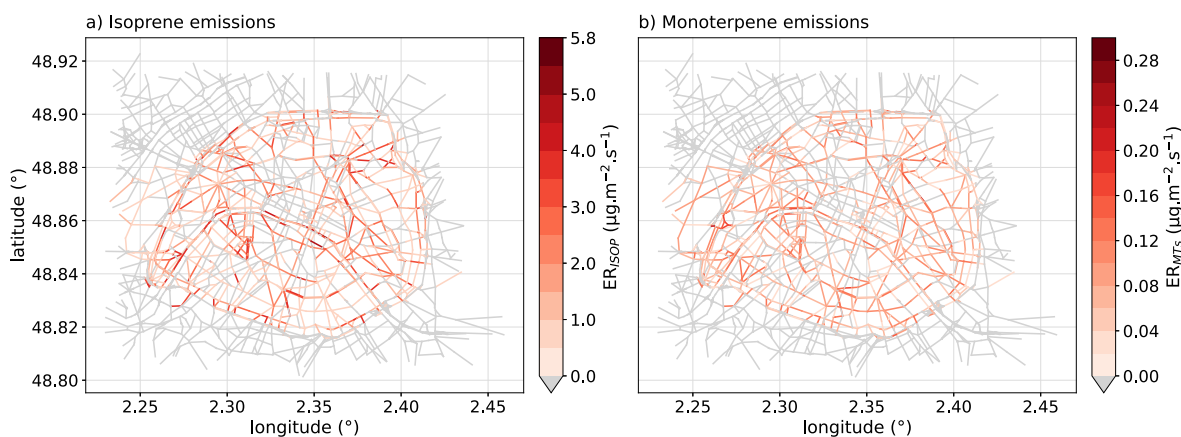


Fig. 1. Maps of temporal average of a) isoprene and b) monoterpene emissions over the 2-month period.

Table 1

Description of the MUNICH simulations performed with the simulated period, the tree effect(s) considered and the corresponding background concentrations (see Maison et al. (2024)).

Simulation name	Start and end dates	Aero. effect	Dry dep. on leaves	Urban tree biogenic emissions	CHIMERE background simulation
REF	06/06–31/07	–	–	–	REF
AERO	13/06–26/06	Yes	–	–	REF
DEP	13/06–26/06	–	Yes	–	REF
BVOC	13/06–26/06	–	–	Yes	bioparis
EFF	06/06–31/07	Yes	Yes	Yes	bioparis
REF TX2	06/06–31/07	–	–	–	REF-TX2
EFF TX2	06/06–31/07	Yes	Yes	Yes $ER_{MT\&SQT} \times 2$	bioparis-TX2

stations with measured compounds is presented in Table S5 and located in the map in Fig. S1.

3. Results and discussion

3.1. Reference simulation

To quantify the tree effects on concentrations, a reference simulation is performed without urban tree, neither at the regional nor local scale. A comparison of observed and simulated concentrations through the average and standard deviation of concentrations along with statistical indicators is summarized in Table S6.

Table S6 shows that the NO_2 concentrations are rather well estimated with a good correlation, a low bias and a NAD lower than 0.3 as recommended by Hanna and Chang (2012). $\text{PM}_{2.5}$ concentrations are also rather well simulated by the model, but PM_{10} are largely underestimated. This may be due the high uncertainties on non-exhaust emissions that affect coarse particle concentrations (Lugon et al., 2021). Isoprene and monoterpene concentrations are also largely underestimated by the model. It may be due to the missing biogenic emissions of urban trees that will be added in this study. The fraction of

organic $\text{PM}_{2.5}$ (organic matter, OM) is also underestimated. As they are formed by condensation of BVOCs, their concentrations are expected to increase with the addition of the local urban biogenic emissions.

In the next sections, the impact of the different individual and overall tree effects is quantified by comparing the concentrations of isoprene, monoterpenes, NO_2 , O_3 , $\text{PM}_{2.5}$, and OM. The average concentrations with all tree effects (3EFF) are compared to the reference simulations without tree (REF) (8 weeks between 06/06 and 31/07/22). This comparison is done with default biogenic emission factors, and with terpene emission factors multiplied by 2 (TX2 scenario) in the supplementary materials. For that comparison, the simulation 3EFF TX2 is compared to the reference simulation REF TX2, i.e. terpene emissions are multiplied by 2 not only for urban trees, but also for the vegetation outside Paris.

The Mean Relative Difference (MRD in %, see Section S11) between the simulation that includes a single tree effect (AERO, DEP, BVOC) and the reference simulation (REF) is also computed during the period from June 13 to 26 (to save computational time) in all the streets of the network and presented in the supplementary materials. In addition, to quantify whether the tree effect on air quality is different during heatwaves, the concentrations are also integrated over heatwave periods. Heatwaves are defined here as days with clear clear-sky conditions and air temperatures reaching 35°C . For the months of June and July 2022, this represents eleven days: June 15 to 18, July 11 to 14 and July 17 to 19.

3.2. Tree effects on isoprene and monoterpene concentrations

Fig. 2 presents the temporal variation of isoprene and monoterpene concentrations measured and simulated at HdV. Hourly averages of measurements are calculated to compare to simulated concentrations.

In the reference simulations (dotted lines), concentrations are very low because anthropogenic isoprene emissions and isoprene background concentrations are low. Isoprene concentrations increase to an order of magnitude close to observations when biogenic emissions from urban trees are included. During the heatwave (from June 15 to 18), concentrations are overestimated by up to a factor 3 probably because isoprene emissions are also overestimated. This was also the case in Maison et al. (2024), where compared to measurements at PRG site (48.82778°N , 2.38056°E), isoprene concentrations are overestimated on June, 16, 17, 19 and 20 but largely underestimated on June 18. As the temperature and global radiation are not overestimated by the model (Fig. S6) and concentrations on other days are rather well simulated, this overestimation might come from the emission parameterizations. In fact, some studies report that the effect of water stress could significantly reduce isoprene emissions during this period (Guenther et al., 2012; Bonn et al., 2019; Otu-Larbi et al., 2020) and is not currently taken into account. It is also important to note that the fragmentation of 2-methyl-

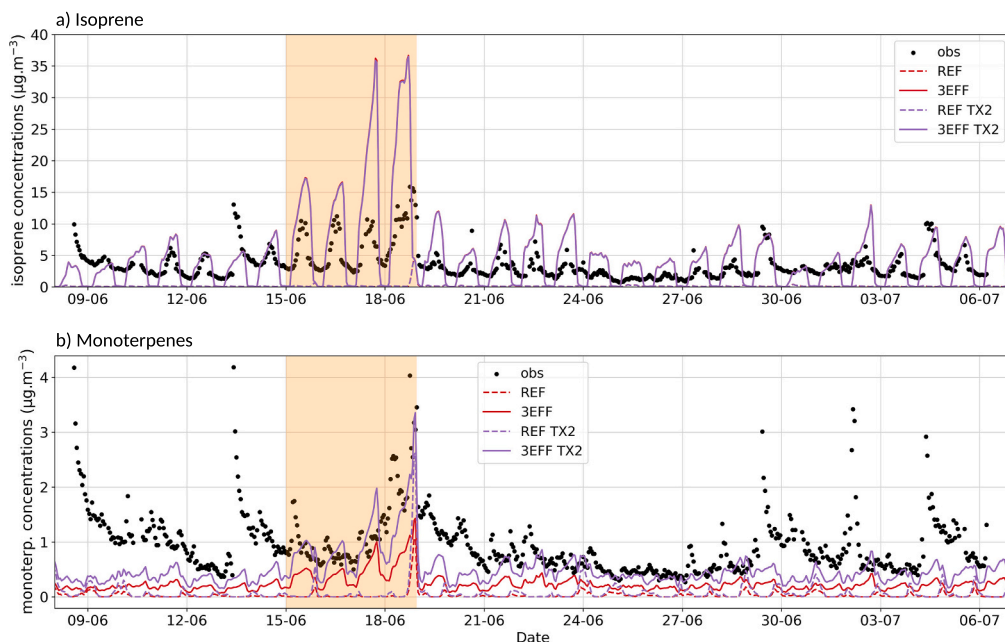


Fig. 2. Hourly evolution of measured (black dots) and simulated with MUNICH (lines) a) isoprene and b) monoterpene concentrations ($\mu\text{g}\cdot\text{m}^{-3}$) in Paris HdV station. Heatwave periods are indicated by orange shaded areas.

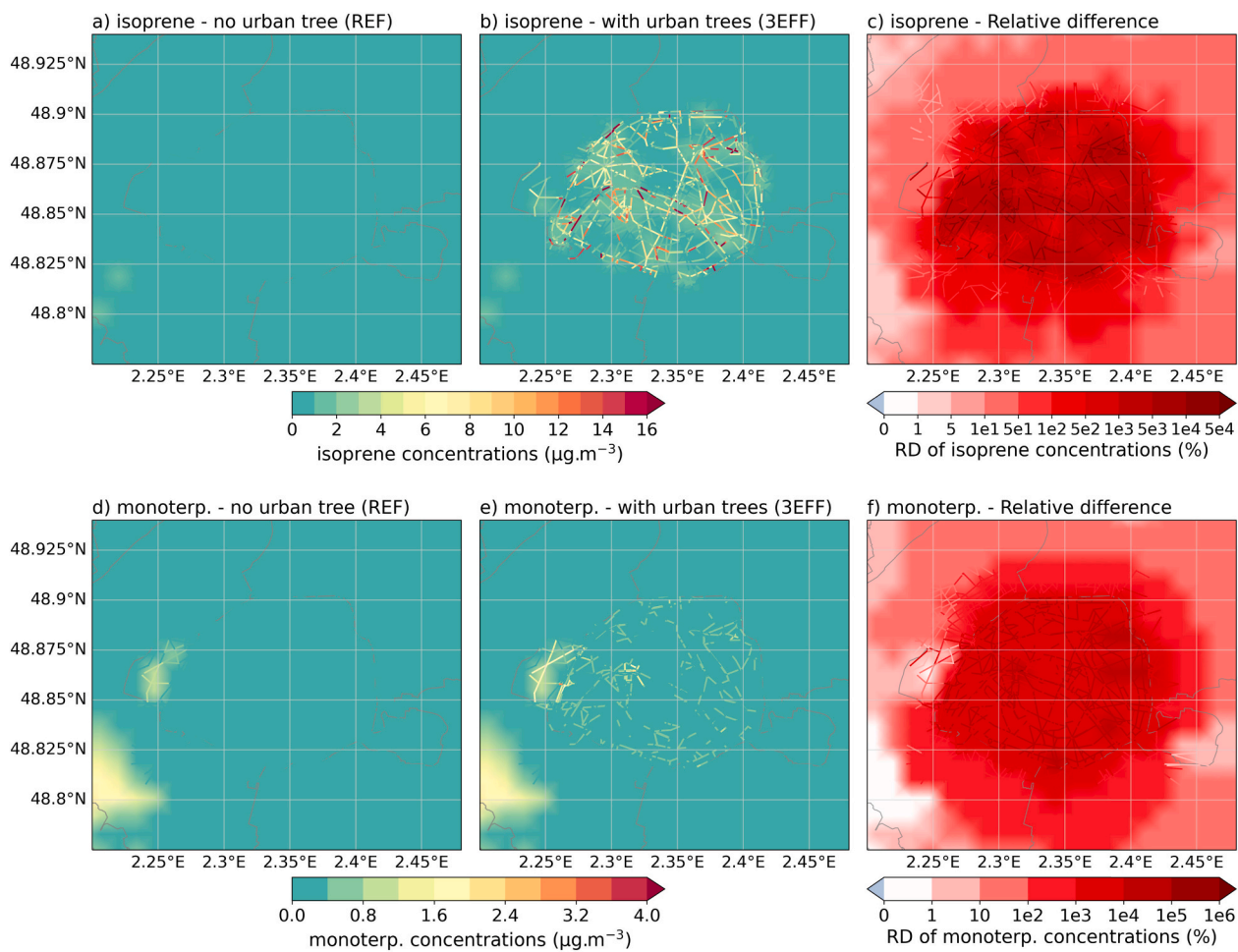


Fig. 3. Average background and street (a, b) isoprene and (d, e) monoterpene concentrations (06/06 to 31/07/22) simulated with CHIMERE/MUNICH (a, d) without trees (REF), (b, e) with trees (3EFF) and (c, f) mean relative difference between the REF and 3EFF (with all tree effects) simulations. (Note that the very large relative differences obtained are due to concentrations in the reference simulation (REF) being close to zero in the denominator.)

3-buten-2-ol (MBO) at m/z 69 (isoprene) was not accounted for, potentially leading to an overestimation of isoprene levels. Besides, the simulated concentrations are much larger during the day than during the night, strongly underestimating the night-time concentrations compared to measurements. The low night-time concentrations in the simulations can be explained by the fact that isoprene is mainly emitted by vegetation during the day and is highly reactive. Further work is therefore needed to identify the cause of the discrepancy between measured and simulated isoprene concentrations at night.

The inclusion of urban trees largely improves the estimation of isoprene concentrations, as shown by the statistical comparison of the simulations with the observations presented in Table S7. The normalized absolute difference (NAD) and the correlation (R) are improved (decrease in NAD from 0.93 to 0.39 and increase in R from 0.35 to 0.64), but the overestimation of isoprene concentrations induced a positive bias (from -3.4 to $+1.0$) and a slightly higher root mean square error (RMSE from 4.2 to 4.9).

A map of the 8-week average isoprene and monoterpene background and street concentrations simulated with CHIMERE/MUNICH with and without trees is presented in Fig. 3.

On average over the 8-week period, taking into account the effects of trees, isoprene concentrations increase very significantly at both the street ($+2690$ %, i.e. $+2.1 \mu\text{g}\cdot\text{m}^{-3}$ on average) and the regional scales (Fig. 3c). This large increase is mainly due to the local isoprene emissions (see Figs. S9 and S10). Dry deposition does not affect isoprene concentrations and the tree aerodynamic effect induces an increase up to $+23$ % and a decrease up to -11 %. The effect of biogenic emissions is larger during heatwave periods (on average $\approx +4,000$ %, i.e. $+3.5 \mu\text{g}\cdot\text{m}^{-3}$ versus $\approx +2,000$ %, i.e. $+1.8 \mu\text{g}\cdot\text{m}^{-3}$ over the 2 weeks of sensitivity analysis, see Fig. S10), because emissions are larger due to higher temperatures and clear-sky conditions (Figs. S6 and S8). Note that there is no difference between the 3EFF and 3EFF TX2 simulations (Figs. 3c and S11c) because unlike monoterpenes and sesquiterpenes, isoprene emissions are the same in the two simulations.

As for isoprene, the concentrations of monoterpenes in the reference simulation are low and underestimated compared to the measurements (Fig. 2b). The addition of local monoterpene emissions from urban trees allows to better simulate the observed concentrations, especially when monoterpene concentrations are doubled in TX2 scenario (decrease in RMSE from 1.0 to 0.7, NAD from 0.85 to 0.35 and bias from -0.9 to -0.5 , and increase in R from 0.25 to 0.35, see Table S8). The concentration peak during the heatwave around the 18th of June is rather well simulated by MUNICH. However concentration increases on the 8th, 13th, 29th of June and 2nd, 4th of July are not simulated by the model. Overall, as there are also uncertainties in monoterpene measurements, the monoterpene concentrations are reasonably well simulated with the TX2 scenario.

The monoterpene concentrations of the REF simulation are very low without urban trees except in western Paris, around the Boulogne wood and the forests of southwestern Paris (Fig. 3d). The addition of urban trees, and mainly monoterpene emissions, increase very largely the concentrations both in the streets ($+9776$ %, i.e. $+0.15 \mu\text{g}\cdot\text{m}^{-3}$ on average) and the background, as shown in Fig. 3e and f. As for isoprene, this increase is mainly due to the addition of biogenic emissions ($+9559$ %, i.e. $+0.13 \mu\text{g}\cdot\text{m}^{-3}$ on the 2-week sensitivity analysis) since there is no dry deposition on leaves and the aerodynamic effect of trees leads to a variation of monoterpene concentrations between -15 % and $+11$ % (Figs. S12 and S13). The increase is larger during heatwaves ($\approx +20,000$ %, i.e. $+0.23 \mu\text{g}\cdot\text{m}^{-3}$ on average) due to higher emissions (Fig. S13). In the TX2 scenario, as monoterpene emissions are doubled, monoterpene concentrations are much higher (Fig. S11e). The relative impact of urban trees is also a little higher especially inside Paris city ($\approx +16,000$ %, i.e. $+0.29 \mu\text{g}\cdot\text{m}^{-3}$ on average in streets, see Fig. S11f). This comparison suggests that monoterpenes concentrations are very sensitive to local emissions. It would therefore be important to reduce uncertainties in emission factors, and also to quantify and characterize

the missing trees in Paris (~ 30 %) and its suburbs.

Biogenic concentrations are, as expected, largely increased by the addition of biogenic emissions from urban trees. The next section focuses on the impact of trees on NO_2 and O_3 concentrations.

3.3. Tree effects on NO_2 and O_3 concentrations

The overall tree effects on NO_2 and O_3 concentrations are evaluated for the 2-month average concentrations in Fig. 4. It presents the 8-week average NO_2 concentrations without trees along with the relative difference between the REF and 3EFF simulations (Fig. 4a and b). The trees induce mainly a variation of NO_2 concentrations in the streets from -17 % to $+36$ %.

To analyse the impacts of urban trees on NO_2 concentrations, the relative impact of each individual tree effect is quantified over the Paris street network on average over 14 days and shown in Fig. S14, and during the 4-day heatwave in Fig. S15. The predominant tree impact that affects NO_2 concentrations is the aerodynamic effect (Figs. S14 and S15). Depending on the street, it leads to an increase up to $+37$ %, but also to a decrease, which can reach -12 % (Fig. S14b). This effect is especially significant in the streets including trees (Fig. S15b). The effect of dry deposition of NO_2 on tree leaves leads to a decrease of concentrations up to -2.5 %, and it is not significant at the city scale (p -value of the t -test between the simulation with trees and the reference simulation ≥ 0.1 , see Fig. S15). Although biogenic emissions, particularly isoprene, can have an impact on NO_2 concentrations through the ozone cycle, this effect is low, as shown by the mean relative difference of the BVOC and the REF simulation, which does not exceed ± 1 % (Fig. S14d). The impact of trees on NO_2 concentrations is therefore related to the aerodynamic effect and it is not much impacted by either the heatwave (Fig. S15) or the TX2 scenario (Fig. S16). Besides, the increase in NO_2 concentrations is rather well correlated with the street LAI, which is the main tree characteristic involved in the aerodynamic effect (Fig. S4a). Besides, the effect of adding trees on the model's performance in simulating NO_2 concentrations depends on the street, but on average it tends to increase the model's overestimation (NAD = 0.20, bias = $2.3 \mu\text{g}\cdot\text{m}^{-3}$ and $R = 0.54$).

Because NO_2 is emitted in streets by traffic, its dispersion is limited by the presence of trees. In order to quantify the possible links between the NO_2 emission intensity and the amplitude of the tree aerodynamic effect, the temporal average of the mean relative difference of the NO_2 concentrations between the simulations AERO and REF (MRD AERO) is plotted as a function of the street LAI and of the NO_2 emissions in Fig. 5. It shows that in treeless streets ($\text{LAI}_{\text{street}} = 0$), the MRD AERO is globally between ± 10 % and seems quite independent of the intensity of emissions. This variability observed in treeless streets could be a consequence of transport of concentrations between adjacent streets. In streets where NO_2 emissions are low, the tree aerodynamic effect is relatively low (between about $+5$ and -10 %) for all LAIs. When NO_2 emissions are higher, a strong aerodynamic effect proportional to LAI is observed. Other factors influence the aerodynamic effect, such as the street aspect ratio and the direction of the wind compared to the street. However, on average over the period, the aerodynamic effect is always significant in high-traffic streets when the LAI exceeds 0.5, and in medium-traffic streets when the LAI exceeds $1.0 \text{m}_{\text{leaf}}^2 \cdot \text{m}_{\text{street}}^{-2}$. The tree aerodynamic effect has an impact on the street concentration, because of emissions of primary pollutants in streets.

Fig. 4c and d shows a comparison of average O_3 concentrations with and without trees over the 8-week simulations. Urban trees lead to a few percent increase in background O_3 concentrations, as shown in Maison et al. (2024). At street level, when the aerodynamic effect of trees is considered, O_3 concentrations decrease as NO_2 concentrations increase. The difference with the TX2 scenario is not clearly visible on the Fig. S16d, and the doubled monoterpene and sesquiterpenes emissions only induce a slightly higher impact of trees on O_3 concentrations. This

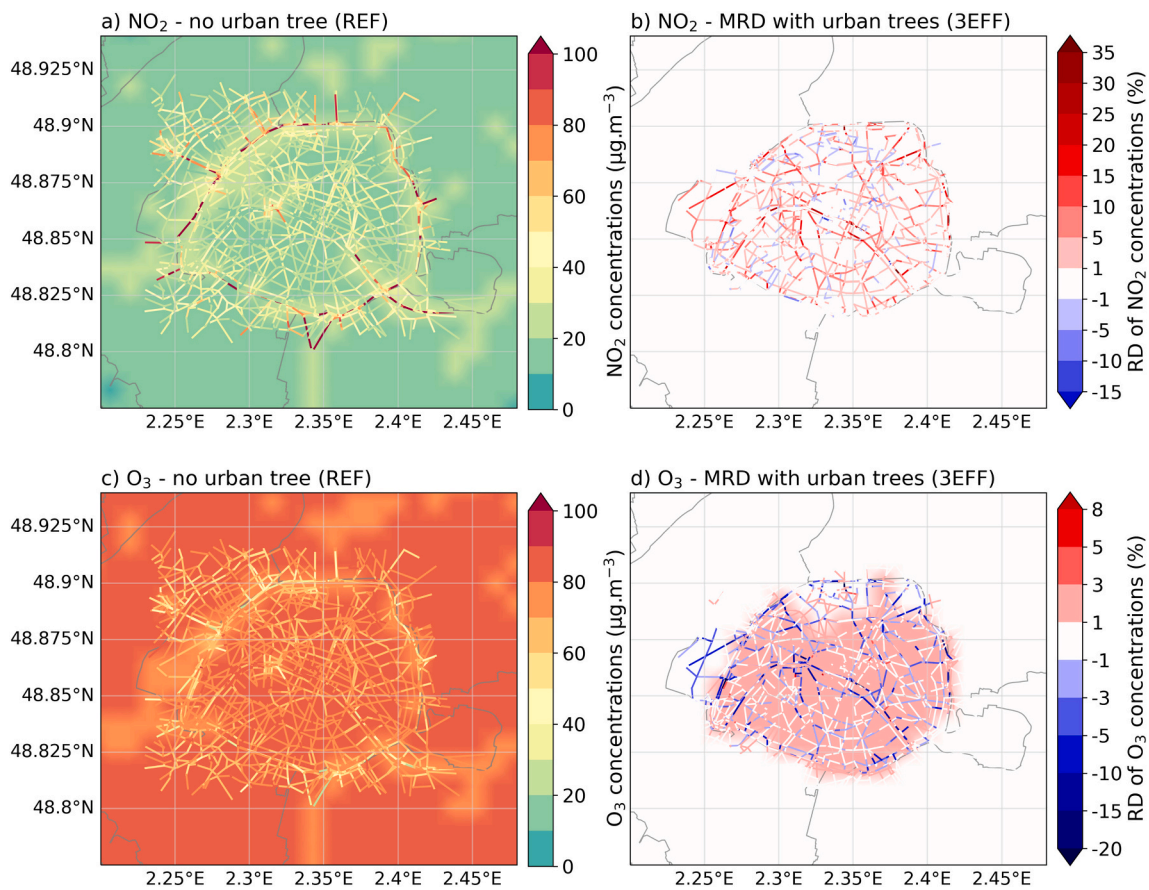


Fig. 4. Average background and street a) NO_2 and c) O_3 concentrations (06/06 to 31/07/22) simulated with CHIMERE/MUNICH without trees (REF) and (b, d) mean relative difference between the REF and 3EFF (with all tree effects) simulations.

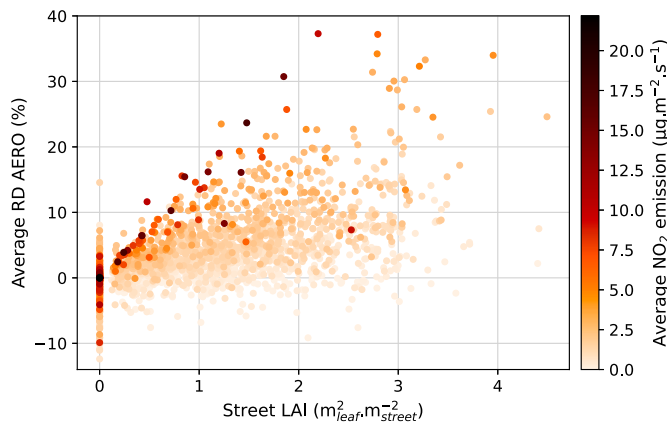


Fig. 5. Mean relative difference of NO_2 concentrations between the simulations AERO and REF as a function of the street LAI and the average NO_2 emission (for each street averaged from 13 to 26/06).

suggests that terpenes have a low impact on O_3 compared to other VOCs such as isoprene, which are emitted in larger quantities.

The individual impacts of urban trees on O_3 concentrations at the street scale are shown in Figs. S17 and S18. The aerodynamic effect leads to a decrease in O_3 concentrations in many streets (up to -23%) and to an increase in others (up to $+17\%$). This effect is more significant in streets containing trees and is anti-correlated with the increase in NO_2 concentrations, as shown in Fig. S19 that plots the MRD AERO of O_3 depending on the MRD AERO of NO_2 . The effect of the dry deposition on O_3 concentrations is very low and does not exceed -2.5% . However,

Fig. S18b shows that the dry deposition is more significant in the streets with trees (-0.62% on average and up to -2.5%). The biogenic emissions induce an average O_3 increase of $+1\%$ which is very homogeneous over the Paris city highlighting the impact of the background concentrations. This increase is larger during the heatwave period ($+2.1\%$) as shown in Fig. S18. As this is a relative difference and the reference simulation (without tree) already includes the effect of weather on O_3 formation, this increase of concentration during the heatwave is only due to the increase of biogenic emissions. The comparison of the individual tree effects with the overall effects (3EFF simulation) shows that the three tree effects compensate each other to give an average tree impact that can be negative, nil or positive depending on the street and time period.

Following the study of gaseous species, the impact of trees on particles, and more specifically on the organic fraction, is quantified in the next section.

3.4. Tree effects on particle concentrations

As the BVOCs emitted by trees may be oxidized leading to the formation of organic particles, called organic matter (OM), the concentrations of these latter may increase because of the urban biogenic emissions. To compare with observations, the OM concentration is computed by summing the concentrations of the organic compounds of particles of diameters lower than $2.5\ \mu\text{m}$.

The hourly-average measured concentrations of OM at the HdV station are compared with simulated concentrations in Fig. 6. It shows that, both for the unmodified and TX2 emission scenarios, the concentrations of the simulations with all tree effects (solid lines) are slightly higher than the concentrations of the reference simulations (dotted

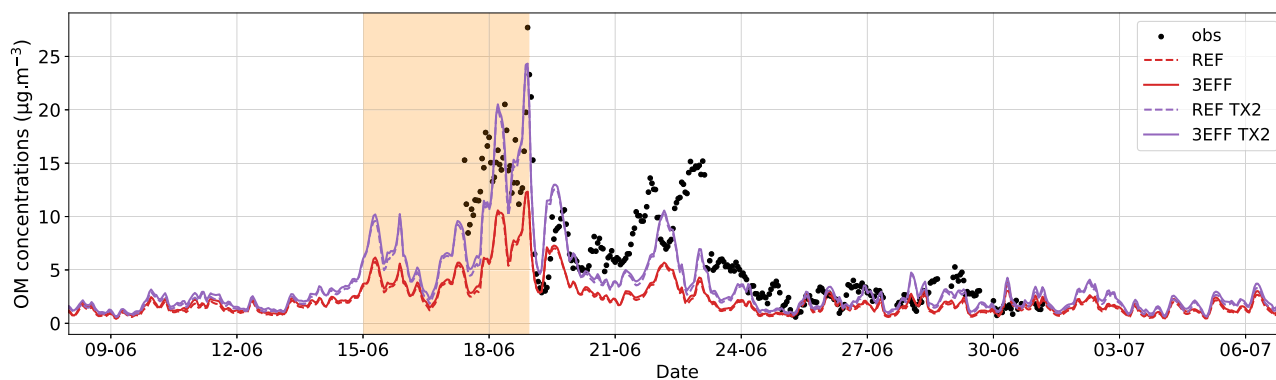


Fig. 6. Hourly evolution of measured (black dots) and simulated with MUNICH (lines) organic matter (OM) concentrations ($\mu\text{g}\cdot\text{m}^{-3}$) in Paris HdV station. Heatwave periods are indicated by orange shaded areas.

lines). Urban trees contribute significantly to the increase in OM concentrations (on average in the street of the HdV station by 11.5 % and 10.1 % for TX2). When monoterpene and sesquiterpene emissions are doubled, the simulated concentrations (red lines) compare much better to observations, especially during the concentration peak around the 18th of June. The statistical comparison of simulations and observations presented in Table S9 shows that the inclusion of urban trees slightly improves the comparison to observations (decrease in bias from -1.5 to -1.3 for TX2). The best agreement between observed and simulated concentrations is in the TX2 scenario, suggesting that the modeled OM concentrations are significantly affected by the terpene concentrations. As simulated terpene concentrations are very sensitive to urban trees, those need to be better characterized to improve the modeling of OM in

summer.

Fig. 7a and b presents the average overall tree effect on OM over the 8 weeks of simulation. It shows that the overall effect of urban trees leads to an increase in OM concentration of +3.9 % on average in Paris streets (Fig. 7a and b). With the TX2 scenario, this increase reaches +4.4 % (Fig. S20b).

Similarly to the previous chemical species studied, the tree effect on OM concentrations is quantified by calculating and mapping the mean relative difference of the sensitivity simulations with the reference simulation (Fig. S21) and by comparing the different MRD over the whole period and the 4-day heatwave (Fig. S22). Fig. S21 shows that the tree aerodynamic effect leads to an increase in OM concentrations mainly in street with trees (up to +31.5 %) and to a decrease in others

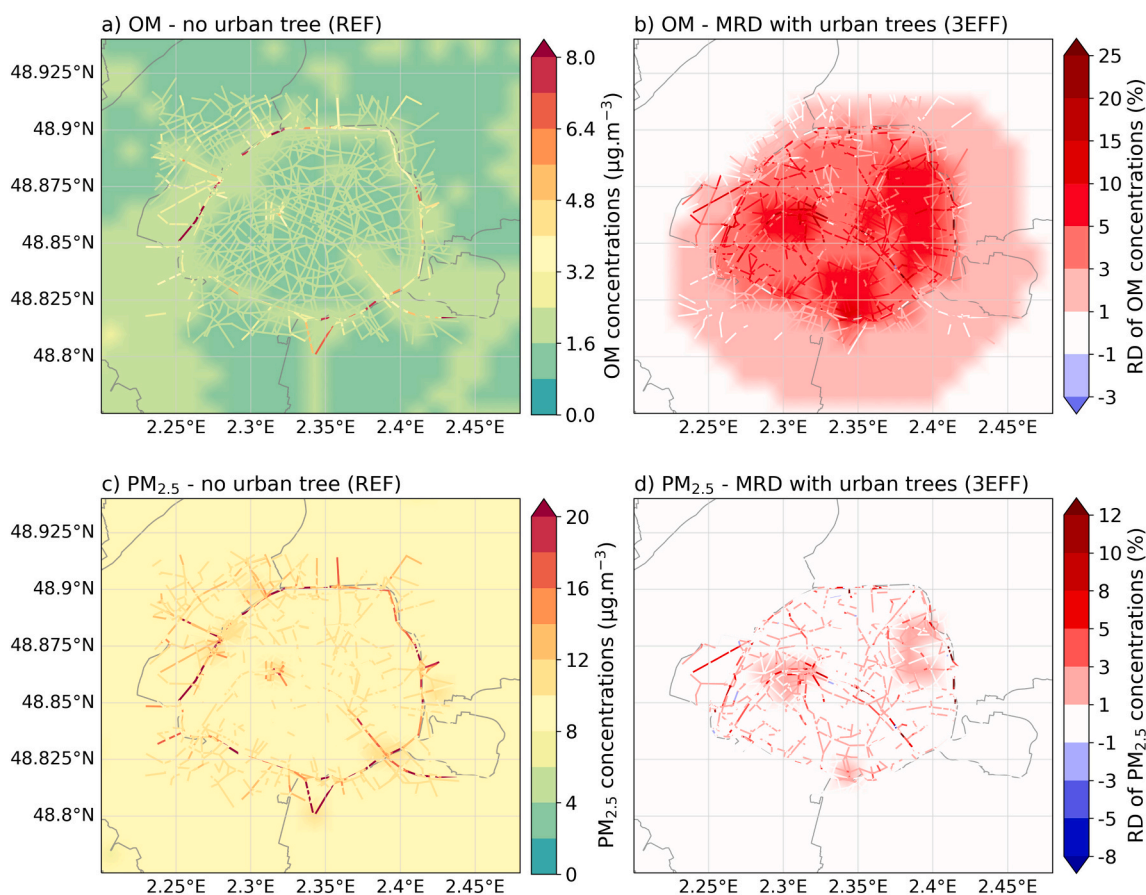


Fig. 7. Average background and street a) OM and c) $\text{PM}_{2.5}$ concentrations (06/06 to 31/07/22) simulated with CHIMERE/MUNICH without trees (REF) and (b, d) mean relative difference between the REF and 3EFF (with all tree effects) simulations.

(up to -7.3%). It is mainly the primary organic aerosols (POAs), emitted by traffic, whose concentrations are increased by the aerodynamic effect of trees. The comparison of the BVOC simulation with the reference shows that OM concentrations are increased quite uniformly across Paris city by on average $+2.4\%$ and up to $+12.3\%$, because the transformation of BVOCs into condensables that may form particles occurs mostly in the urban background (Wang et al., 2023). During the heatwave period, this OM increase reaches $+3.4\%$ on average and up to $+21.3\%$. The dry deposition of OM on leaves remains limited (up to -2.4%) and non-significant compared to the other effects, in particular biogenic emissions.

Fig. 7c and d shows the average overall tree effect on $PM_{2.5}$ over the 8 weeks of simulation. The increase in $PM_{2.5}$ due to biogenic emissions is visible locally in the background concentrations over area with denser vegetation (up to $+1.6\%$). In streets, $PM_{2.5}$ concentrations vary from -8.4% to $+21.7\%$ and increase by $+0.8\%$ on average. Doubling monoterpene and sesquiterpene emissions (TX2) leads to an increase of $PM_{2.5}$ concentrations of $+1.2\%$ on average in all streets (Fig. S20c and d).

If the individual effects of the trees are considered, the aerodynamic effect of trees induces a large increase in $PM_{2.5}$ concentrations in some streets (up to $+22\%$) and a small decrease in others (up to -5%) (Figs. S23b and S24). A part of $PM_{2.5}$ are emitted by traffic, so like NO_2 , they are sensitive to the presence of trees in streets and to the emission intensity, which explains the heterogeneity obtained. Although biogenic urban tree emissions strongly influence OM concentrations, they have a limited impact on $PM_{2.5}$ concentrations ($+0.5\%$ on average) except in the densely vegetated areas (up to $+2.9\%$) (Fig. S23d). The effect of dry deposition on leaves is weak and induces a decrease of $PM_{2.5}$ concentrations by up to -1.6% (Fig. S23c). Note that the addition of trees does not significantly modify the statistics between simulated and observed $PM_{2.5}$.

To summarise, $PM_{2.5}$ concentrations increase because of biogenic emissions from urban trees and in particular monoterpene and sesquiterpene emissions that leads to the formation of OM. In addition, there is an increase in concentrations in streets with trees due to the aerodynamic effect and a small decrease in adjacent streets.

4. Conclusion

The three main effects of trees, i.e. reduced ventilation (aerodynamic effect), dry deposition on leaves and biogenic emissions are rarely all taken into account over large urban areas (Mircea et al., 2023). This study aims to estimate the urban tree effects on air quality at the street and city scale, which to our knowledge, has never been studied before. Firstly, the three main effects of urban trees on air quality were added to the modeling chain CHIMERE/MUNICH: aerodynamic effect in street canyons, dry-deposition on leaves, BVOC emissions.

The simulations show that the dry deposition reduces the concentrations of gas and particles by at most a few percents. This decrease is only slightly significant for ozone in streets with trees. The tree aerodynamic effect affects mainly the species emitted in streets. The impact of aerodynamic effect increases with emission intensity and tree LAI. It is significant in streets with high and medium emissions depending on the LAI, and reaches $+37\%$ for NO_2 . Although ozone is a secondary pollutant, and is therefore not emitted in the street, concentrations are also modified by the aerodynamic effect of trees, because of the increase in NO_x concentrations and titration. The tree aerodynamic effect also impacts OM and $PM_{2.5}$ concentrations through the effect on primary aerosols (up to $+31.5$ and $+22\%$ respectively).

As expected, the biogenic emissions from urban trees increase very largely the concentrations of isoprene and monoterpenes both in the streets and the background. This increase is higher during heatwaves due to higher emissions. Compared with measurements, isoprene concentrations are globally well estimated, but they tend to be overestimated during the heatwave. However, for monoterpenes and

sesquiterpenes, the scenario where their emissions are doubled leads to the best correlation between simulated and observed monoterpene concentrations. The urban tree biogenic emissions do not significantly impact NO_2 concentrations and induce a slight increase in O_3 street concentrations of 1% on average over the 14 days and of 2.1% during the 4-day heatwave. The OM concentrations significantly increase because of biogenic emissions ($+2.4\%$ on average over the 14 days and $+3.4\%$ during the heatwave). This increase is larger when monoterpene and sesquiterpene emissions are doubled, and this scenario gives a better comparison to measurements. This suggests the importance of monoterpenes and sesquiterpenes from urban vegetation in the formation of OM in summer.

To summarise, this study indicates that trees cannot be considered as an effective solution for reducing air pollution via leaf deposition. However, there are large uncertainties in the dry deposition parameterizations used and more measurements of dry-deposition velocities on urban trees at the leaf scale are necessary. The aerodynamic effect locally increases the concentrations of the species emitted in the street. Its intensity depends on tree LAI and its impact on concentrations is correlated to chemical species emission, suggesting that the plantation of large trees in streets with heavy traffic should be limited. Finally, the biogenic emissions induce an increase in ozone (mainly due to isoprene and OVOC emissions) and organic matter (also due to monoterpene and sesquiterpene emissions), especially during the heatwave periods. It should be remembered, that there is a large uncertainty on the emission factors of BVOCs (about a factor of 2) and they vary with the tree species. Emission factors are not specifically estimated for urban trees, which can be quite different from forests, as they are planted and pruned artificially. Therefore, the impact of urban trees on ozone and particulate concentrations varies greatly from one city to another (Owen et al., 2003; Calfapietra et al., 2013; Ren et al., 2017). More measurements of emission factors specific to urban trees are needed to lower down the uncertainties on tree BVOC emission factors, and in particular terpenes. The overestimation of isoprene concentrations observed could be due to the effect of water stress on trees, which could reduce isoprene emissions, and it is not considered in this study.

Trees have a significant impact on air quality, notably through their aerodynamic effects and BVOC emissions. The conclusions of this study can be generalized at least to cities whose climate and morphology (building aspect ratio) are similar to those of Paris. The modeling chain developed could be used to study different tree planting scenarios to see whether certain tree species and configurations could limit these impacts. Given the many positive aspects of urban trees (effects on thermal comfort, water, biodiversity, well being, etc.), planting trees in cities is essential, but urban tree management should include criteria related to air quality (Sicard et al., 2018), which is not the case today.

Code availability

The code to process the Paris tree inventory database, calculate tree characteristics and estimate biogenic emissions is available online at: <https://zenodo.org/doi/10.5281/zenodo.10381923>, last accessed on 02/02/2024 (Maison et al., 2023).

The version of CHIMERE-WRF code used here is available on request.

The last version of the MUNICH source code is available online at: <https://doi.org/10.5281/zenodo.4168984>, last accessed on 02/02/2024.

CRediT authorship contribution statement

Alice Maison: Writing – review & editing, Writing – original draft, Visualization, Validation, Software, Methodology, Investigation, Formal analysis, Conceptualization. **Lya Lugon:** Writing – review & editing, Visualization, Validation, Software, Investigation, Formal analysis. **Soo-Jin Park:** Writing – review & editing, Validation, Software, Investigation, Formal analysis. **Christophe Boissard:** Writing – review & editing,

Resources, Investigation, Funding acquisition, Data curation. **Aurélien Fauchaux**: Writing – review & editing, Resources, Investigation, Data curation. **Valérie Gros**: Writing – review & editing, Resources, Investigation, Funding acquisition, Data curation. **Carmen Kalalian**: Writing – review & editing, Resources, Investigation, Data curation. **Youngseob Kim**: Writing – review & editing, Software, Resources, Methodology. **Juliette Leymarie**: Writing – review & editing, Funding acquisition. **Jean-Eudes Petit**: Writing – review & editing, Resources, Investigation, Data curation. **Yelva Roustan**: Writing – review & editing, Software, Methodology. **Olivier Sanchez**: Writing – review & editing, Resources, Data curation. **Alexis Squarconi**: Writing – review & editing, Software, Methodology. **Myrto Valari**: Writing – review & editing, Software, Methodology. **Camille Viatte**: Writing – review & editing, Resources, Data curation. **Jérémy Vigneron**: Writing – review & editing, Resources, Investigation, Data curation. **Andrée Tuzet**: Writing – review & editing, Funding acquisition, Conceptualization. **Karine Sartelet**: Writing – review & editing, Writing – original draft, Validation, Supervision, Software, Project administration, Methodology, Investigation, Funding acquisition, Formal analysis, Conceptualization.

Declaration of competing interest

The authors declare that they have no known competing financial interests or personal relationships that could have appeared to influence the work reported in this paper.

Data availability

VOC hourly concentrations measured at the HdV station are available on the Aeris datacenter at <https://www.aeris-data.fr/catalogue/?uuid=e508b1fd-b0d9-4e26-b6fc-6c3f28f40efc>.

NOx and OM hourly concentrations measured at the HdV station and meteorological data are in the process of being submitted to the Aeris datacenter.

Hourly concentrations measured at the Airparif station are available on the Airparif's Open Data Portal: <https://data-airparif-asso.opendata.arcgis.com/>. Regional and traffic emissions inventory is available on request.

Acknowledgements

This work benefited from the French state aid managed by the sTREEt ANR project (ANR-19-CE22-0012), and by the ANR under the “Investissements d'avenir” program (ANR-11-IDEX-0004-17-EURE-0006) with support from IPSL/Composair. This project has also received funding from the European Union's Horizon 2020 - Research and Innovation Framework Programme under grant agreement No 101036245 (RI-URBANS). This project was provided with computer and storage resources by GENCI at TGCC thanks to the grant A0150114641 on the supercomputer Joliot Curie's the ROME partition.

Appendix A. Supplementary data

Supplementary data to this article can be found online at <https://doi.org/10.1016/j.scitotenv.2024.174116>.

References

- Arnfield, A., 2003. Two decades of urban climate research: a review of turbulence, exchanges of energy and water, and the urban heat island. *Int. J. Climatol.* 23, 1–26. <https://doi.org/10.1002/joc.859>.
- Baghi, R., Helmig, D., Guenther, A., Duhl, T., Daly, R., 2012. Contribution of flowering trees to urban atmospheric biogenic volatile organic compound emissions. *Biogeosciences* 9, 3777–3785. <https://doi.org/10.5194/bg-9-3777-2012>. URL: <https://bg.copernicus.org/articles/9/3777/2012/>.
- Berkowicz, R., 2000. OSPM - a parameterised street pollution model. *Environ. Monit. Assess.* 65, 323–331. <https://doi.org/10.1023/A:1006448321977>.
- Berland, A., 2017. The role of trees in urban stormwater management. *Landsc. Urban Plan.* 162, 167–177. <https://doi.org/10.1016/j.landurbplan.2017.02.017>.
- Bonn, B., Magh, R.K., Rombach, J., Kreuzwieser, J., 2019. Biogenic isoprenoid emissions under drought stress: different responses for isoprene and terpenes. *Biogeosciences* 16, 4627–4645. <https://doi.org/10.5194/bg-16-4627-2019>. URL: <https://bg.copernicus.org/articles/16/4627/2019/>.
- Buccolieri, R., Gromke, C., Di Sabatino, S., Ruck, B., 2009. Aerodynamic effects of trees on pollutant concentration in street canyons. *Sci. Total Environ.* 407, 5247–5256. <https://doi.org/10.1016/j.scitotenv.2009.06.016>. URL: <https://linkinghub.elsevier.com/retrieve/pii/S0048969709005944>.
- Buccolieri, R., Salim, S.M., Leo, L.S., Di Sabatino, S., Chan, A., Ielpo, P., de Gennaro, G., Gromke, C., 2011. Analysis of local scale tree-atmosphere interaction on pollutant concentration in idealized street canyons and application to a real urban junction. *Atmos. Environ.* 45, 1702–1713. <https://doi.org/10.1016/j.atmosenv.2010.12.058>. URL: <https://linkinghub.elsevier.com/retrieve/pii/S1352231011000057>.
- Calfapietra, C., Fares, S., Manes, F., Morani, A., Sgrigna, G., Loreto, F., 2013. Role of biogenic volatile organic compounds (BVOC) emitted by urban trees on ozone concentration in cities: a review. *Environ. Pollut.* 183, 71–80. <https://doi.org/10.1016/j.envpol.2013.03.012>. URL: <https://www.sciencedirect.com/science/article/pii/S0269749113001310>.
- Canaval, E., Millet, D.B., Zimmer, I., Nosenko, T., Georgii, E., Partoll, E.M., Fischer, L., Alwe, H.D., Kulmala, M., Karl, T., Schnitzler, J.P., Hansel, A., 2020. Rapid conversion of isoprene photooxidation products in terrestrial plants. *Communications Earth & Environment* 1, 44. <https://doi.org/10.1038/s43247-020-00041-2>. URL: <https://www.nature.com/articles/s43247-020-00041-2>.
- Carruthers, D., Edmunds, H., Lester, A., McHugh, C., Singles, R., 2000. Use and validation of ADMS-urban in contrasting urban and industrial locations. *Int. J. Environ. Pollut.* 14, 364–374. <https://doi.org/10.1504/IJEP.2000.000558>.
- Escobedo, F.J., Nowak, D.J., 2009. Spatial heterogeneity and air pollution removal by an urban forest. *Landsc. Urban Plan.* 90, 102–110. <https://doi.org/10.1016/j.landurbplan.2008.10.021>. URL: <https://www.sciencedirect.com/science/article/pii/S0169204608001801>.
- Fenger, J., 1999. Urban air quality. *Atmos. Environ.* 33, 4877–4900. [https://doi.org/10.1016/S1352-2310\(99\)00290-3](https://doi.org/10.1016/S1352-2310(99)00290-3). URL: <https://www.sciencedirect.com/science/article/pii/S1352231099002903>.
- Fu, R., Paden, I., García-Sánchez, C., 2024. Should we care about the level of detail in trees when running urban microscale simulations? *Sustain. Cities Soc.* 101, 105143. <https://doi.org/10.1016/j.scs.2023.105143>. URL: <https://www.sciencedirect.com/science/article/pii/S2210670723007527>.
- Gromke, C., Blocken, B., 2015. Influence of avenue-trees on air quality at the urban neighborhood scale. Part II: traffic pollutant concentrations at pedestrian level. *Environ. Pollut.* 196, 176–184. <https://doi.org/10.1016/j.envpol.2014.10.015>. URL: <https://linkinghub.elsevier.com/retrieve/pii/S0269749114004382>.
- Gromke, C., Ruck, B., 2007. Influence of trees on the dispersion of pollutants in an urban street canyon-experimental investigation of the flow and concentration field. *Atmos. Environ.* 41, 3287–3302. <https://doi.org/10.1016/j.atmosenv.2006.12.043>. URL: <https://www.sciencedirect.com/science/article/pii/S1352231007000076>.
- Guenther, A., Hewitt, C.N., Erickson, D., Fall, R., Geron, C., Graedel, T., Harley, P., Klinger, L., Lerdau, M., McKay, W., Pierce, T., Scholes, B., Steinbrecher, R., Tallamraju, R., Taylor, J., Zimmerman, P., 1995. A global model of natural volatile organic compound emissions. *J. Geophys. Res.* 100, 8873–8892. <https://doi.org/10.1029/94JD02950>.
- Guenther, A., Jiang, X., Heald, C.L., Sakulyanontvittaya, T., Duhl, T., Emmons, L.K., Wang, X., 2012. The model of emissions of gases and aerosols from nature version 2.1 (MEGAN2.1): an extended and upyear framework for modeling biogenic emissions. *Geosci. Model Dev.* 5, 1471–1492. <https://doi.org/10.5194/gmd-5-1471-2012>. URL: <https://gmd.copernicus.org/articles/5/1471/2012/>.
- Hami, A., Abdi, B., Zarehaghi, D., Maulan, S.B., 2019. Assessing the thermal comfort effects of green spaces: a systematic review of methods, parameters, and plants' attributes. *Sustain. Cities Soc.* 49, 101634. <https://doi.org/10.1016/j.scs.2019.101634>. URL: <https://linkinghub.elsevier.com/retrieve/pii/S2210670718327306>.
- Hanna, S., Chang, J., 2012. Acceptance criteria for urban dispersion model evaluation. *Meteorol. Atmos. Phys.* 116, 133–146. <https://doi.org/10.1007/s00703-011-0177-1>.
- Hicks, B., Baldocchi, D., Meyers, T., Hosker, R., Matt, D., 1987. A preliminary multiple resistance routine for deriving dry deposition velocities from measured quantities. *Water Air Soil Pollut.* 36, 311–330. <https://doi.org/10.1007/BF00229675>.
- Jeanjean, A.P.R., Monks, P.S., Leigh, R.J., 2016. Modelling the effectiveness of urban trees and grass on PM2.5 reduction via dispersion and deposition at a city scale. *Atmos. Environ.* 147, 1–10. <https://doi.org/10.1016/j.atmosenv.2016.09.033>. URL: <https://www.sciencedirect.com/science/article/pii/S1352231016307336>.
- Karl, T., Harley, P., Emmons, L., Thornton, B., Guenther, A., Basu, C., Turnipseed, A., Jardine, K., 2010. Efficient atmospheric cleansing of oxidized organic trace gases by vegetation. *Science* 330, 816–819. <https://doi.org/10.1126/science.1192534>.
- Kim, Y., Wu, Y., Seigneur, C., Roustan, Y., 2018. Multi-scale modeling of urban air pollution: development and application of a street-in-grid model (v1.0) by coupling MUNICH (v1.0) and polair3d (v1.8.1). *Geosci. Model Dev.* 11, 611–629. <https://doi.org/10.5194/gmd-11-611-2018>. URL: <https://www.geosci-model-dev.net/11/611/2018/>.
- Kim, Y., Lugon, L., Maison, A., Sarica, T., Roustan, Y., Valari, M., Zhang, Y., André, M., Sartelet, K., 2022. MUNICH v2.0: a street-network model coupled with SSH-aerosol (v1.2) for multi-pollutant modelling. *Geosci. Model Dev.* 15, 7371–7396. <https://doi.org/10.5194/gmd-15-7371-2022>. URL: <https://gmd.copernicus.org/articles/15/7371/2022/>.

- Kusaka, H., Kondo, H., Kikigawa, Y., Kimura, F., 2001. A simple single-layer urban canopy model for atmospheric models: comparison with multi-layer and slab models. *Bound.-Layer Meteorol.* 101, 329–358. <https://doi.org/10.1023/A:1019207923078>.
- Kuttler, W., 2008. The urban climate – basic and applied aspects. In: Marzluff, J.M., Shulenberg, E., Endlicher, W., Alberti, M., Bradley, G., Ryan, C., Simon, U., ZumBrunnen, C. (Eds.), *Urban Ecology: An International Perspective on the Interaction Between Humans and Nature*. Springer US, pp. 233–248. https://doi.org/10.1007/978-0-387-73412-5_13.
- Lindén, J., Gustafsson, M., Uddling, J., Watne, A., Plejeh, H., 2023. Air pollution removal through deposition on urban vegetation: the importance of vegetation characteristics. *Urban For. Urban Gree.* 81, 127843. <https://doi.org/10.1016/j.ufug.2023.127843>. URL: <https://www.sciencedirect.com/science/article/pii/S1618866723000146>.
- Livesley, S.J., McPherson, E.G., Calfapietra, C., 2016. The urban forest and ecosystem services: impacts on urban water, heat, and pollution cycles at the tree, street, and city scale. *J. Environ. Qual.* 45, 119–124. <https://doi.org/10.2134/jeq2015.11.0567>.
- Lugon, L., Sartelet, K., Kim, Y., Vigneron, J., Chrétien, O., 2020. Nonstationary modeling of NO₂, NO and NO_x in Paris using the street-in-grid model: coupling local and regional scales with a two-way dynamic approach. *Atmos. Chem. Phys.* 20, 7717–7740. <https://doi.org/10.5194/acp-20-7717-2020>. URL: <https://acp.copernicus.org/articles/20/7717/2020/>.
- Lugon, L., Vigneron, J., Debert, C., Chrétien, O., Sartelet, K., 2021. Black carbon modeling in urban areas: investigating the influence of resuspension and non-exhaust emissions in streets using the street-in-grid model for inert particles (sing-inert). *Geosci. Model Dev.* 14, 7001–7019. <https://doi.org/10.5194/gmd-14-7001-2021>.
- Lyons, T., Kenworthy, J., Newman, P., 1990. Urban structure and air pollution. *Atmospheric Environment. Part B. Urban Atmosphere* 24, 43–48. [https://doi.org/10.1016/0957-1272\(90\)90008-I](https://doi.org/10.1016/0957-1272(90)90008-I). URL: <https://linkinghub.elsevier.com/retrieve/pii/095712729090008I>.
- Maison, A., Flageul, C., Carissimo, B., Tuzet, A., Sartelet, K., 2022a. Parametrization of horizontal and vertical transfers for the street-network model MUNICH using the CFD model code saturne. *Atmosphere* 13, 527. <https://doi.org/10.3390/atmos13040527>. URL: <https://www.mdpi.com/2073-4433/13/4/527>.
- Maison, A., Flageul, C., Carissimo, B., Wang, Y., Tuzet, A., Sartelet, K., 2022b. Parametrizing the aerodynamic effect of trees in street canyons for the street network model MUNICH using the CFD model code saturne. *Atmos. Chem. Phys.* 22, 9369–9388. <https://doi.org/10.5194/acp-22-9369-2022>. URL: <https://acp.copernicus.org/articles/22/9369/2022/>.
- Maison, A., Lugon, L., Kim, Y., Park, S.J., Tuzet, A., Sartelet, K., 2023. Characterization of Urban Trees and Calculation of Their Bvoc Emissions. Zenodo. <https://doi.org/10.5281/zenodo.10381923>.
- Maison, A., Lugon, L., Park, S.J., Baudic, A., Cantrell, C., Couvidat, F., D'Anna, B., Di Biagio, C., Gratien, A., Gros, V., Kalalian, C., Kammer, J., Michoud, V., Petit, J.E., Shahin, M., Simon, L., Valari, M., Vigneron, J., Tuzet, A., Sartelet, K., 2024. Significant impact of urban tree biogenic emissions on air quality estimated by a bottom-up inventory and chemistry transport modeling. *Atmos. Chem. Phys.* 24, 6011–6046. <https://doi.org/10.5194/acp-24-6011-2024>. URL: <https://acp.copernicus.org/articles/24/6011/2024/>.
- Masson, V., Lemonsu, A., Hidalgo, J., Voogt, J., 2020. Urban climates and climate change. *Annu. Rev. Environ. Resour.* 45, 411–444. <https://doi.org/10.1146/annurev-environ-012320-083623>.
- McHugh, C., Carruthers, D., Edmunds, H., 1997. ADMS and ADMS-urban. *Int. J. Environ. Pollut.* 8, 438–440. <https://doi.org/10.1504/IJEP.1997.028193>.
- McPherson, E.G., van Doorn, N.S., Peper, P.J., 2016. Urban Tree Database and Allometric Equations. Technical Report PSW-GTR-253. U.S. Department of Agriculture, Forest Service, Pacific Southwest Research Station. <https://doi.org/10.2737/PSW-GTR-253>. URL: <https://www.fs.usda.gov/tree-search/pubs/52933>.
- Meek, D.W., Hatfield, J.L., Howell, T.A., Idso, S.B., Reginato, R.J., 1984. A generalized relationship between photosynthetically active radiation and solar radiation. *Agron. J.* 76, 939–945. <https://doi.org/10.2134/agronj1984.00021962007600060018x>.
- Menut, L., Bessagnet, B., Briant, R., Cholakan, A., Couvidat, F., Mailler, S., Pennel, R., Siour, G., Tuccella, P., Turquety, S., Valari, M., 2021. The CHIMERE v2020r1 online chemistry-transport model. *Geosci. Model Dev.* 14, 6781–6811. <https://doi.org/10.5194/gmd-14-6781-2021>. URL: <https://gmd.copernicus.org/articles/14/6781/2021/>.
- Méziani, M., Vauléon, Y.F., Blancot, C., Besse, M.T., Bruneau, F., Alba, D., 2013. Étude sur le potentiel de végétalisation des toitures terrasses à Paris. Technical Report. URL: http://www.apur.org/sites/default/files/documents/publication/documents-associés/végétalisation_toitures_terrasses.pdf?to ken=pLvYHox. (Accessed 26 May 2024).
- Mircea, M., Borge, R., Finardi, S., Briganti, G., Russo, F., de la Paz, D., D'Isidoro, M., Cremona, G., Villani, M.G., Cappellietti, A., Adani, M., D'Elia, I., Piersanti, A., Sorrentino, B., Petralia, E., de Andrés, J.M., Narros, A., Silibello, C., Pepe, N., Prandi, R., Carlino, G., 2023. The role of vegetation on urban atmosphere of three European cities. Part 2: evaluation of vegetation impact on air pollutant concentrations and depositions. *Forests* 14, 1255. <https://doi.org/10.3390/f14061255>. URL: <https://www.mdpi.com/1999-4907/14/6/1255>.
- Municipality of Paris, 2023. Paris Data: Les arbres. <https://opendata.pari.fr/explore/dataset/les-arbres/>. (Accessed 3 March 2023).
- Nemitz, E., Vieno, M., Carnell, E., Fitch, A., Steadman, C., Cryle, P., Holland, M., Morton, R.D., Hall, J., Mills, G., Hayes, F., Dickie, I., Carruthers, D., Fowler, D., Reis, S., Jones, L., 2020. Potential and limitation of air pollution mitigation by vegetation and uncertainties of deposition-based evaluations. *Philos. Trans. R. Soc. A Math. Phys. Eng. Sci.* 378, 20190320. <https://doi.org/10.1098/rsta.2019.0320>.
- Ng, N.L., Herndon, S.C., Trimbom, A., Canagaratna, M.R., Croteau, P.L., Onasch, T.B., Sueper, D., Worsnop, D.R., Zhang, Q., Sun, Y.L., Jayne, J.T., 2011. An aerosol chemical speciation monitor (ACSM) for routine monitoring of the composition and mass concentrations of ambient aerosol. *Aerosol Sci. Technol.* 45, 780–794. <https://doi.org/10.1080/02786826.2011.560211>.
- Nguyen, T.B., Crounse, J.D., Teng, A.P., St. Clair, J.M., Paulot, F., Wolfe, G.M., Wennberg, P.O., 2015. Rapid deposition of oxidized biogenic compounds to a temperate forest. *Proc. Natl. Acad. Sci.* 112. <https://doi.org/10.1073/pnas.1418702112>.
- Niinemets, U., Loreto, F., Reichstein, M., 2004. Physiological and physicochemical controls on foliar volatile organic compound emissions. *Trends Plant Sci.* 9, 180–186. <https://doi.org/10.1016/j.tplants.2004.02.006>. URL: <https://www.sciencedirect.com/science/article/pii/S1360138504000524>.
- Nowak, D.J., Crane, D.E., Stevens, J.C., 2006. Air pollution removal by urban trees and shrubs in the United States. *Urban For. Urban Gree.* 4, 115–123. <https://doi.org/10.1016/j.ufug.2006.01.007>. URL: <https://linkinghub.elsevier.com/retrieve/pii/S1618866706000173>.
- Nunez, M., Oke, T.R., 1977. The energy balance of an urban canyon. *J. Appl. Meteorol. Climatol.* 16, 11–19. [https://doi.org/10.1175/1520-0450\(1977\)016<0011:TEBOAU>2.0.CO;2](https://doi.org/10.1175/1520-0450(1977)016<0011:TEBOAU>2.0.CO;2). URL: https://journals.ametsoc.org/view/journals/apme/16/1/1520-0450.1977.016.0011.teboau_2.0_co_2.xml.
- Oke, T.R., Mills, G., Christen, A., Voogt, J.A., 2017. *Urban Climates*. Cambridge University Press. <https://doi.org/10.1017/9781139016476>.
- Otu-Larbi, F., Bolas, C.G., Ferracci, V., Staniaszek, Z., Jones, R.L., Malhi, Y., Harris, N.R.P., Wild, O., Ashworth, K., 2020. Modelling the effect of the 2018 summer heatwave and drought on isoprene emissions in a UK woodland. *Glob. Chang. Biol.* 26, 2320–2335. <https://doi.org/10.1111/gcb.14963>.
- Owen, S.M., MacKenzie, A.R., Stewart, H., Donovan, R., Hewitt, C.N., 2003. Biogenic volatile organic compound (VOC) emission estimates from an urban tree canopy. *Ecol. Appl.* 13, 927–938. <https://doi.org/10.1890/01-5177>.
- Pigeon, G., Legain, D., Durand, P., Masson, V., 2007. Anthropogenic heat release in an old European agglomeration (Toulouse, France). *Int. J. Climatol.* 27, 1969–1981. <https://doi.org/10.1002/joc.1530>.
- Powers, J.G., Klemp, J.B., Skamarock, W.C., Davis, C.A., Dudhia, J., Gill, D.O., Coen, J.L., Gochis, D.J., Ahmadov, R., Peckham, S.E., et al., 2017. The weather research and forecasting model: overview, system efforts, and future directions. *Bull. Am. Meteorol. Soc.* 98, 1717–1737. <https://doi.org/10.1175/BAMS-D-15-00308.1>.
- Ren, Y., Qu, Z., Du, Y., Xu, R., Ma, D., Yang, G., Shi, Y., Fan, X., Tani, A., Guo, P., Ge, Y., Chang, J., 2017. Air quality and health effects of biogenic volatile organic compounds emissions from urban green spaces and the mitigation strategies. *Environ. Pollut.* 230, 849–861. <https://doi.org/10.1016/j.envpol.2017.06.049>. URL: <https://www.sciencedirect.com/science/article/pii/S0269749117309491>.
- Roeland, S., Moretti, M., Amorim, J.H., Branquinho, C., Fares, S., Morelli, F., Niinemets, U., Paoletti, E., Pinho, P., Sgrigna, G., Stojanovski, V., Tiwary, A., Sicard, P., Calfapietra, C., 2019. Towards an integrative approach to evaluate the environmental ecosystem services provided by urban forest. *J. For. Res.* 30, 1981–1996. <https://doi.org/10.1007/s11676-019-00916-x>.
- Sailor, D.J., Georgescu, M., Milne, J.M., Hart, M.A., 2015. Development of a national anthropogenic heating database with an extrapolation for international cities. *Atmos. Environ.* 118, 7–18. <https://doi.org/10.1016/j.atmosenv.2015.07.016>.
- Santiago, J.L., Borge, R., Martin, F., de la Paz, D., Martilli, A., Lumbreras, J., Sanchez, B., 2017. Evaluation of a CFD-based approach to estimate pollutant distribution within a real urban canopy by means of passive samplers. *Sci. Total Environ.* 576, 46–58. <https://doi.org/10.1016/j.scitotenv.2016.09.234>. URL: <https://www.sciencedirect.com/science/article/pii/S0048969716321647>.
- Sartelet, K., Couvidat, F., Wang, Z., Flageul, C., Kim, Y., 2020. SSH-aerosol v1.1: a modular box model to simulate the evolution of primary and secondary aerosols. *Atmosphere* 11, 525. <https://doi.org/10.3390/atmos11050525>. URL: <https://www.mdpi.com/2073-4433/11/5/525>.
- Selmi, W., Weber, C., Rivière, E., Blond, N., Mehdi, L., Nowak, D., 2016. Air pollution removal by trees in public green spaces in Strasbourg City, France. *Urban For. Urban Gree.* 17, 192–201. <https://doi.org/10.1016/j.ufug.2016.04.010>. URL: <https://linkinghub.elsevier.com/retrieve/pii/S1618866716301571>.
- Setälä, H., Viippola, V., Rantalainen, A.L., Pennanen, A., Yli-Pelkonen, V., 2013. Does urban vegetation mitigate air pollution in northern conditions? *Environ. Pollut.* 183, 104–112. <https://doi.org/10.1016/j.envpol.2012.11.010>. URL: <https://www.sciencedirect.com/science/article/pii/S0269749112004885>.
- Sicard, P., Agathokleous, E., Araminiene, V., Carrari, E., Hoshika, Y., De Marco, A., Paoletti, E., 2018. Should we see urban trees as effective solutions to reduce increasing ozone levels in cities? *Environ. Pollut.* 243, 163–176. <https://doi.org/10.1016/j.envpol.2018.08.049>. URL: <https://www.sciencedirect.com/science/article/pii/S026974911831813X>.
- Soulhac, L., Salizzoni, P., Cierco, F.X., Perkins, R., 2011. The model SIRANE for atmospheric urban pollutant dispersion; part I, presentation of the model. *Atmos. Environ.* 45, 7379–7395. <https://doi.org/10.1016/j.atmosenv.2011.07.008>. URL: <https://linkinghub.elsevier.com/retrieve/pii/S1352231011007096>.
- Soulhac, L., Salizzoni, P., Mejean, P., Didier, D., Rios, I., 2012. The model SIRANE for atmospheric urban pollutant dispersion; PART II, validation of the model on a real case study. *Atmos. Environ.* 49, 320–337. <https://doi.org/10.1016/j.atmosenv.2011.11.031>. URL: <https://linkinghub.elsevier.com/retrieve/pii/S1352231011012143>.
- Soulhac, L., Nguyen, C., Volta, P., Salizzoni, P., 2017. The model SIRANE for atmospheric urban pollutant dispersion. PART III: validation against NO₂ yearly concentration measurements in a large urban agglomeration. *Atmos. Environ.* 167, 377–388.

- <https://doi.org/10.1016/j.atmosenv.2017.08.034>. URL: <https://linkinghub.elsevier.com/retrieve/pii/S1352231017305472>.
- Stocker, J., Hood, C., Carruthers, D., McHugh, C., 2012. ADMS-urban: developments in modelling dispersion from the city scale to the local scale. *Int. J. Environ. Pollut.* 50, 308–316. <https://doi.org/10.1504/IJEP.2012.051202>.
- Taha, H., 1997. Urban climates and heat islands: albedo, evapotranspiration, and anthropogenic heat. *Energ. Buildings* 25, 99–103. [https://doi.org/10.1016/S0378-7788\(96\)00999-1](https://doi.org/10.1016/S0378-7788(96)00999-1). URL: <https://www.sciencedirect.com/science/article/pii/S0378778896009991>.
- Taleghani, M., 2018. Outdoor thermal comfort by different heat mitigation strategies- a review. *Renew. Sust. Energ. Rev.* 81, 2011–2018. <https://doi.org/10.1016/j.rser.2017.06.010>. URL: <https://linkinghub.elsevier.com/retrieve/pii/S1364032117309474>.
- Venkatram, A., Pleim, J., 1999. The electrical analogy does not apply to modeling deposition of particles. *Atmos. Environ.* 33, 3075–3076. [https://doi.org/10.1016/S1352-2310\(99\)00094-1](https://doi.org/10.1016/S1352-2310(99)00094-1).
- Vos, P.E., Mailheu, B., Vankerkom, J., Janssen, S., 2013. Improving local air quality in cities: to tree or not to tree? *Environ. Pollut.* 183, 113–122. <https://doi.org/10.1016/j.envpol.2012.10.021>. URL: <https://linkinghub.elsevier.com/retrieve/pii/S0269749112004605>.
- Walmsley, J., Wesely, M., 1996. Modification of coded parametrizations of surface resistances to gaseous dry deposition. *Atmos. Environ.* 30, 1181–1188. [https://doi.org/10.1016/1352-2310\(95\)00403-3](https://doi.org/10.1016/1352-2310(95)00403-3).
- Wang, Y., Flageul, C., Maison, A., Carissimo, B., Sartelet, K., 2023. Impact of trees on gas concentrations and condensables in a 2-D street canyon using CFD coupled to chemistry modeling. *Environ. Pollut.*, 121210 <https://doi.org/10.1016/j.envpol.2023.121210>. URL: <https://www.sciencedirect.com/science/article/pii/S0269749123002129>.
- Wesely, M., 1989. Parameterization of surface resistances to gaseous dry deposition in regional-scale numerical models. *Atmos. Environ.* 23, 1293–1304. <https://doi.org/10.1016/j.atmosenv.2007.10.058>.
- Xing, Y., Brimblecombe, P., 2019. Role of vegetation in deposition and dispersion of air pollution in urban parks. *Atmos. Environ.* 201, 73–83. <https://doi.org/10.1016/j.atmosenv.2018.12.027>. URL: <https://www.sciencedirect.com/science/article/pii/S1352231018308847>.
- Xu, W., Croteau, P., Williams, L., Canagaratna, M., Onasch, T., Cross, E., Zhang, X., Robinson, W., Worsnop, D., Jayne, J., 2017. Laboratory characterization of an aerosol chemical speciation monitor with PM_{2.5} measurement capability. *Aerosol Sci. Technol.* 51, 69–83. <https://doi.org/10.1080/02786826.2016.1241859>.
- Yang, J., Shi, B., Shi, Y., Marvin, S., Zheng, Y., Xia, G., 2020. Air pollution dispersal in high density urban areas: research on the triadic relation of wind, air pollution, and urban form. *Sustain. Cities Soc.* 54, 101941 <https://doi.org/10.1016/j.scs.2019.101941>. URL: <https://www.sciencedirect.com/science/article/pii/S2210670719322474>.
- Zhang, L., Gong, S., Padro, J., L., B., 2001. A size-segregated particle dry deposition scheme for an atmospheric aerosol module. *Atmos. Environ.* 35, 549–560. [https://doi.org/10.1016/S1352-2310\(00\)00326-5](https://doi.org/10.1016/S1352-2310(00)00326-5).
- Zhang, L., Moran, M.D., Makar, P.A., Brook, J.R., Gong, S., 2002. Modelling gaseous dry deposition in AURAMS: a unified regional air-quality modelling system. *Atmos. Environ.* 36, 537–560. [https://doi.org/10.1016/S1352-2310\(01\)00447-2](https://doi.org/10.1016/S1352-2310(01)00447-2). URL: <https://linkinghub.elsevier.com/retrieve/pii/S1352231001004472>.
- Zhang, L., Brook, J.R., Vet, R., 2003. A revised parameterization for gaseous dry deposition in air-quality models. *Atmos. Chem. Phys.* 16 <https://doi.org/10.5194/acp-3-2067-2003>.